Synthetic gel particle formation for acoustofluidic applications

Thibaut Valery

2022

LUND
UNIVERSITY

Master's Thesis in Biomedical Engineering

Faculty of Engineering LTH
Department of Biomedical Engineering

Supervisor: Richard Soller
Examiner: Per Augustsson

Abstract

Cancer cell detection by particle sorting systems is a very challenging field which could help to discover cancers at an earlier stage. Acoustophoresis used as a particle sorting system is based on the difference between the acoustic properties of particles and the medium. Using a standing acoustic wave, the particles with the equivalent acoustic properties are focused at the same point in the channel. During the experiments on acoustophoresis systems some parameters can be adjusted such as the flow rate, the concentration, the frequency of the acoustic wave, etc. Microparticles such as silica-based, polystyrene and PMMA particles are mainly used as test particles to replace the cells. Artificial test particles have more defined properties enabling to repeat under the same conditions all experiments and have an easier handling. However, these particles are not reproducing very accurately the acoustic properties of human cells. Ideally, the test particles should have the same size and have acoustic properties as close to the cells that we want to investigate as possible. The work carried out in this project has been oriented around gel particles as a solution to replace the particles found on the market that are used as test particles in acoustofluidic systems. Agarose gel particles within the size range of the human cells have been produced using different microfluidic droplet generator chips. The gel particles was tested in acoustophoresis devices in a water medium and they interacted with the acoustic field. The smallest particles with a diameter of about $7-10\ \mu m$ were circulating around in the vortices of the acoustic streaming. Some other gel particles had a motion towards the anti-node. Even if a real behavior of the particles in the water buffer has not been determined, it points to a possible way of producing gel test particles for a further use in acoustofluidic systems.

Popular science

Producing gel particles to mimic human cells in an acoustofluidic system.

Acoustofluidics is a promising technique to move particles with a sound wave. This sound wave applies a force to particles in a suspension. This force is directed in the cross section of the channel. This technique is particularly promising for cancer cells detection. Because the particles can be moved in the lateral direction, different outlet at the end of the fluidic chip could allow to increase the concentration of the cancer cells if they are focused in the same place. This increasing concentration could allow to detect some cancers at earlier stage that are not visible with standard techniques because the amount of cancer cells would be too low for the detection. In the development of this technique different particles are used to mimic the cell behavior when the acoustic force is applied to them. No commercially available particles are manufactured for the specific use of mimicking the cell behavior in an acoustofluidic system. The main test particles used are polystyrene beads. However their properties are not fully able to mimic completely the acoustic properties of cells. Indeed, these particles are not soft enough compared to the cells and this hardness implies that they feel a different acoustic force than the cells. The idea of this project is to produce a new type of particles that could mimic the acoustic cell properties and replace the polystyrene beads. This work focused on the production of agarose gel particles. The agarose is a sugar and when it is mixed with water it forms a gel structure. This gel structure is softer than polystyrene and could provide better results regarding the cell mimicking. The agarose gel particles were formed by using a droplet generator chip to get spherical test particles. Once produced these gel test particles were collected and tested in the acoustofluidic system. The gel particles interacted with the acoustic wave and moved in the channel when the acoustic force was applied however further measurements are still needed to investigate if their properties mimic the cells as expected.

Acknowledgements

First of all, I would like to thank my supervisor Richard Soller and my examiner Per Augustsson for giving me the opportunity to work on this project. It has been a real pleasure to work with you and to learn along your sides. Thank you again for your help throughout this project. Thank you Enrico Corato for the precious help on different experiments you set up for me. Wei Qiu and Ola Jakobsson, thank you for your advice and your help. Finally, I would like to thank Anna Fornell for the valuable discussion about droplet formation.

I also want to thank everyone from the Department of Biomedical Engineering. It has been a real pleasure to meet you and talk to you. I really had a great time working in the department on my project.

Jules Reniaud, thank you a lot for backing me up when I needing and for the great time we had struggling together. The same goes for Linda Péroux, Damien Gautier and Fred Celle, thank you all for the great moments we shared all together.

Contents

Symbol	Description	Unit
F_{rad}	Radiation force	N
Φ	Contrast factor	-
a	Radius of the particle	m
E_{ac}	Acoustic energy density	Pa
$\tilde{\kappa}$	Compressibility ratio between the particle and the medium	-
$\tilde{\rho}$	Density ratio between the particle and the medium	-
Ca	Capillary number	-
Re	Reynolds number	-
μ	dynamic viscosity	$Pa.s$
Q	flow rate	$m^3.s^{-1}$
V_I	injector volume	m^3
γ	interfacial tension	$N.m^{-1}$
v	flow velocity	$m.s^{-1}$
$v_{particle}$	velocity of the particle	$m.s^{-1}$
ρ	density	$kg.m^{-3}$
g	gravity	$m.s^{-2}$
R_{in}	inner diameter of the needle	m
R_{out}	outer diameter of the needle	m
$V_{droplet}$	droplet volume	m^3
R	ball radius	m

1 Introduction

1.1 Acoustophoresis phenomenon

Acoustophoresis is a phenomenon that allows to sort particles depending on different parameters such as size, density and compressibility. An acoustic wave generated by a piezo resonator propagates along the perpendicular axis of a microfluidic chip filled with a fluid. The resulting standing acoustic wave generates an acoustic force F_{rad} on the particles circulating in the flow **Fig. 1(a)**. This force depends on the radius a of the particle and the difference between the acoustic properties (density ρ and compressibility κ) of the particles (index p) relative to the medium (index m) **[1]**. This force allows for instance to increase the concentration of the particles **Fig. 1(b)** or clean a solution from some particles **Fig. 1(c)**. The contrast factor Φ given in eq. (**2**) resulting from the ratio of compressibilities ($\tilde{\kappa} = \frac{\kappa_p}{\kappa_m}$) and densities ($\tilde{\rho} = \frac{\rho_p}{\rho_m}$) between the particles and the medium can be positive or negative. The particles with a positive contrast factor are driven to the node(s) of the acoustic wave in the perpendicular axis of the channel (the center of the channel for a standing acoustic half-wave) while the particles with a negative contrast factor are pushed to the anti-node(s), generally the walls. The acoustic force depends both on the contrast factor and on the size of the particles as shown in eq. (**1**). The bigger the particle is the stronger the force and the faster the particles move to the node or the anti-node. Indeed, the behaviour of the particles whether they move to the node or the anti-node is very dependent of the medium. Which means two particles cannot necessarily be separated with any medium. However, the size, or any acoustic property can also be a discrimination factor. If the travel time of the particles to the center node due to the radiation force is different enough, particles can be sorted even though the two different particles are driven to the same point in the channel **Fig. 1(d)**. The velocity of the particles depends also on the Stoke's drag Force which is shown in eq. (**3**), valid for small Reynolds number and spherical particles. This force is directed towards the opposite direction of the movement of the particle slowing down the particles.

$$F_{rad} = \frac{4}{3}\pi\Phi a^3 k_y E_{ac} sin(k_y y)\overrightarrow{e_y} \tag{1}$$

$$\Phi = 1 - \tilde{\kappa} + \frac{3(\tilde{\rho} - 1)}{2\tilde{\rho} + 1} \tag{2}$$

$$F_{stoke} = 6\pi\eta r v_{particle} \tag{3}$$

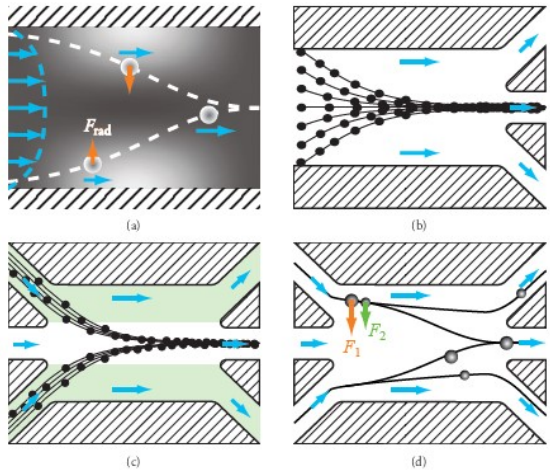

Figure 1: Illustration of **(a)** the radiation force to move particles in the perpendicular axis of the flow. **(b)** This system can enrich a solution with particles, **(c)** move particles to another fluid and **(d)** separate particles with different intrinsic acoustic properties. Reproduced from **[1]** with permission from Per Augustsson.

As the behaviour of the particles depends on the medium, either they are pushed to the node or the anti-node, it is possible to create different focusing points to increase the possibilities for the sorting. That is the principle of the iso-acoustic focusing (IAF) **[2]**. An iodixanol concentration gradient flow is used to create a gradient in the medium properties across the channel. When the particle moves across the channel, its contrast factor changes due to a change in the medium properties. It results in specific focusing points along the gradient for each type of particles depending on their own properties. Indeed, in a certain concentration of iodixanol, one particle is pushed to the wall/anti-node if the contrast factor is negative (in the case of a half standing acoustic wave, the node is in the center of the channel and the anti-nodes are on the walls). For the next concentration the particle could be dragged to the node/center of the channel, if the contrast factor is positive, leading to an equilibrium on a focus point with a zero contrast factor.

1.2 Droplet formation

Droplet formation is also a major part of this work. To produce the smallest droplets possible and get a steady droplet formation, the droplets must be generated in a dripping mode. This dripping mode shown in Fig. **2** is achieved by adjusting the

flow rates of the dispersed phase (solution making the droplets) and the continuous phase (solution surrounding the droplets).

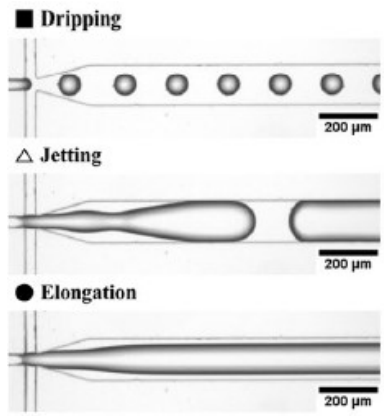

Figure 2: Different modes of droplet generation. **[3]**

The generation of the droplets is ruled by the Laplace pressure estimating the pressure difference $\Delta P_{droplet}$ between the inside and the outside of the droplet. This pressure difference is given by eq. (**4**). It depends on the radius of the droplet R and the interfacial tension γ. The smaller the droplet is the higher the pressure inside. On the contrary, if the interfacial tension between the two fluids decreases, the pressure difference decreases.

$$\Delta P_{droplet} = \gamma \frac{2}{R} \tag{4}$$

For micrometer dimensions in droplet generation, the pressure difference $\Delta P_{droplet}$ between two ends of the channels is already high as it depends roughly on the power of 4 of the dimension R as shown by the Poiseuille eq. (**5**) valid for a cylindrical channels. The length of the channel L and the flow rate Q are also parameters to take into account for the increasing pressure along the channel. Finally the viscosity μ is also a major concern in our study as the pressure inside the channel is meant to be high but the viscosity of the gel that is used might increase even more the pressure. And a high pressure would lead to a higher coefficient of variation in the droplet formation **[4]**.

$$\Delta P_{channel} = \frac{8\mu LQ}{\pi R^4} \tag{5}$$

The size of the droplets formed is lead by the capillary number given in eq. (**6**). It involves the velocity (v) of the flow, the dynamic viscosity (μ) of the fluid but also

the interfacial tension (γ) between the continuous and dispersed phase. As a whole, it relates viscous forces to interfacial tension which are two forces involved in the characterisation of the droplet formation.

$$Ca = \frac{v\mu}{\gamma} \tag{6}$$

1.3 Human cells properties

Microfluidic devices and especially acoustofluidic devices are widely used for human cell sorting and analysis. These devices are very promising for detecting the circulating tumor cells (CTCs) and get an early diagnostic of metastasising cancer. An early diagnosis allows treatment of cancer in its early stage, improving the odds of patient survival.

To be able to sort and detect the tumor cells within acoustofluidic devices, there needs to be a difference in acoustic properties between normal cells and tumor cells. Some acoustic properties of normal cells and tumor cells are shown in the Tab. **1**. The tumor cells given in the Tab. **1** correspond to different types of cancer. The DU-145 cell is a prostate tumor cell. The MCF-7 corresponds to a breast tumor cell. The test particles commonly used in acoustofludics are polystyrene beads and polymethylmethacrylate (PMMA) beads. Their acoustic properties are given in the Tab. **2**.

Cell	Size (μm)	Density (kg/m^{-3})	Compressibility (TPa^{-1})
RBCs	7-8	1101(13)	334(2)
WBCs	6-9	1054(3)	393(1)
DU-145	15-22	1062(1)	384(1)
MCF-7	18-25	1055(1)	373(1)

Table 1: Properties of red (RBCs) and white (WBCs) blood cells compared with DU-145 **[5]** and MCF-7 **[6]** tumor cells.

Particle	Size (μm)	Density (kg/m^{-3})	Compressibility (TPa^{-1})
PS5	5	1058(6)	273(2)
PS7	7	1059(3)	276(3)
PMMA	3	1184(7)	173(6)

Table 2: Properties of the test particles commonly used in acoustofluidic devices. **[7]**

The main observation shows that humans cells and the common test particles used have similar densities but quite different compressibilities. The size of these Polysterene (PS) beads and PMMA beads are quite similar to the human cells. The density of the PS bead is relatively similar to WBCs and the cancer cells mentionned in the Tab. **1** but it differs from the RBCs density. Besides, there is also a shape difference especially between the doughnut shape of the RBCs and the usual spherical shape of the test particles.

1.4 Synthetic particles to mimic the cell properties

Test particles are very convenient to use in acoustofluidic devices as their properties are stable and can be controlled. The experiments can be run under the same conditions (concentration, flow rates, etc.) with the same particle sample. Systems can also be calibrated with known test particles for further use with unknown cells or cells with wider properties for instance. However, there are few choices on the market regarding these test particles. Besides, they are not tunable in their properties for specific use and their compressibility is too low compared to the cells. The cells used in acoustofluidic systems are very time consuming, less stable than synthetic particles and also have varying properties. Hence, there is a need in acoustofluidic to use test particles with tunable, consistent and accurate properties to get rid of the use of cells for the first steps of the researches when their use is not mandatory.

1.4.1 Silica, polystyrene and PMMA microparticles

Microparticles such as silica-based, polystyrene and PMMA particles are mainly used to calibrate or work with microfluidic systems without having to use cells for instance. The problem remains that these particles do not replicate the acoustic cell properties.

The compressibility of these test particles is too low compared to the compressibility of the cells. It happens to be a factor of almost two between both as shown in Tab. **1** and **2**. It implies that the acoustic force which applies to the test particles depends almost exclusively on the difference between the compressibility of the medium and the particles if they have the same size (eq. (**2**)). There are systems such as IAF where cells are separated by the contrast factor. However when replacing cells by test particles to calibrate and validate such methods, one cannot achieve the same contrast factor with the same medium. The particles do not mimic the behavior of the cells in the acoustofluidic system.

1.4.2 Giant unilamellar vesicles (GUVs) formation

GUVs (with a size range of 1-200µm) are interesting particles as they have a similar structure as the human cell membrane which is made up of fatty-acid lipids and proteins. Indeed, GUVs are made by encapsulating a liquid with a lipid layer using for example a double emulsion or a cDICE method **[8]**. The choice of the encapsulated liquid would have well known properties giving the opportunity to tune the acoustic properties of the resulting soft particle. However, the general size of these GUVs are about a hundred of micron and it appears to be difficult to produce at very small size. Some papers show the production of GUVs around 10 microns but with very diverse sizes from the particles produced **[9]**. Besides, the GUVs are very unstable.

1.4.3 Gel-based droplets

Particle with cell-like acoustic properties can be generated with gel-based droplets. Gel droplets are potentially more stable than liposomes and could be produced at smaller dimension. The two types of gel-based particles particularly interesting because easy to produce are agarose-droplets and PEG-droplets. The gels mentioned here are soft but solid material due to a porous structure. It appears in **[10]** that PEG-droplets (transformed into gel using UV-light) are less convenient and stable to produce than agarose-droplets. That is why agarose has been chosen for this study to look into the possibility of making test particles with it.

Agarose is a polysaccharide (carbohydrate polymer) and is generally used as a gel for electrophoresis. The 3D agarose structure is held together by hydrogen bonds. There are different types of agarose (especially regarding the gelling point) but the interesting property is the hysteresis cycle of the gel formation. The melting point is generally higher in temperature than the gelling point of the solution of water and agarose. The a5030 Agarose from Sigma Aldrich has an ultra low gelling point around 8-17°C (manufacturer). The gelling process will be evaluated in **3.1.3**. The gel properties such as the gelling and melting point actually depend on the agarose concentration. The common range of concentration of agarose in water for electrophoresis applications is between 1 and 3%. The gel can be stable over a certain range of temperature below the temperature breaking the hydrogen bonds. Due to their stability, it becomes therefore conceivable to make gel-based droplets with agarose which will be used around ambient temperature. However, it must not exceed a certain temperature to avoid destroying the gel structure.

1.5 Scope of the study

It was shown the interest of having particles that mimic the cells properties, that are tunable, stable and have a small variation of their properties. The goal is to produce and use microparticles that are stable, consistent in their properties and with similar acoustic properties as cells. To achieve this, new types of microparticles must be produced and tested. It was chosen in this study to use agarose gel particles to try to mimic the cell behavior in the acoustofluidic systems. The agarose gel production as well as the droplet formation from the solution are detailed in further sections. The gel particles will also be tested in acoustofluidic systems to evaluate whether they could be good candidates as test particles in this field.

2 Droplet generation

2.1 Oil and surfactant combination

2.1.1 HFE-7500 fluorinated oil as continuous phase

The dispersed phase corresponding to the liquid forming the droplets is an aqueous phase (98% water at least). Which means the continuous phase in which the droplets will be submerged needs to be non-miscible with an aqueous phase. There are different types of oil which could be used. For droplet generation, an effective oil and probably the most widely used is the HFE-7500 fluorinated oil **[11]**, **[12]**. Other types of oil have been experimentally tested in this project without giving as good result as the fluorinated oil. Which is why the HFE-7500 fluorinated oil is used for the droplet generation experiments presented in this thesis.

2.1.2 Surfactant as stabilizer

To get a stable droplet generation in microfluidic devices, the use of a surfactant is mandatory. Besides, it gives much more stability to the droplets generated preventing them to merge if they collide.

A surfactant is a substance lowering the interfacial tension between two liquids. This interesting property referring to the eq. (**4**) allows to decrease the pressure inside the droplet and thus the supplied energy density to form the droplet is lowered. Otherwise, the energy taken from the shear forces to form the droplet would need to be higher which means a high viscosity of the oil or a high flow rate. The surfactant also allows to bind two molecules from two non-miscible solutions together. Surfactant are usually amphiphilic organic compounds which means they are made of one hydrophilic group and one lipophilic group (hydrophobic). The lipophilic group can differ from the type of lipid used.

The emulsifier property of the surfactant is in our case a useful ally as it reduces the interfacial tension between both liquids and stabilise the droplet generation. Indeed, if no surfactant is used the droplets are coming out of the injector by waves as shown in Fig. **3**. Besides, the surfactant also prevents water droplets from merging when they collide. Indeed, the water droplets are surrounded by a lipid layer which is bonded to the water with the organic compounds of the surfactant. This means that the hydrophobic groups of the surfactant surrounding the droplet are directed towards the outside of the droplet. When two droplets collide, the surrounding layers of the droplets repel each other preventing the merging. As one important aspect of the droplet generation is the regular size of the particles, this non-merging

condition is mandatory as two droplets merging would create a bigger one.

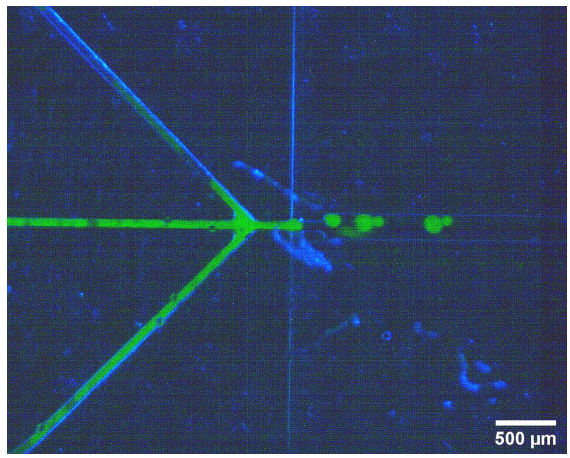

Figure 3: The droplets of water (fluorescent liquid) are generated in fluorinated oil without any surfactant. The chip used is the 162 model from ChipShop with a 70 µm width injector. The droplets come out in the collection channel with different size and nothing prevents them to merge. Besides, waves of droplets are generated due to a high interfacial tension between both solutions. The pressure in the dispersed phase increases when no droplets are formed due to the high interfacial forces and it is released by creating multiple droplets at the same time.

2.2 Theoretical droplet size

The size of the droplet generated depends on several parameters among them the flow rates, the dimensions on the injector and the fluid properties. It is interesting to predict the size of the droplet generated to produce test particles with the desired dimensions. The idea is to check how accurate a theoretical model of the droplet volume can be and if the model is relevant to predict test particles generation.

2.2.1 Theoretical droplet size model

A predictive droplet size model is given by eq. (**7**) for the volume of the droplet generated **[13]**. The volume depends on several parameters from both the dispersed phase (index **d**) and the continuous phase (index **c**). It depends first on the flows and the geometry of the chip with the Reynolds number ($Re = vl/\mu$ with v the velocity

of the flow, l the characteristic length and μ the dynamic viscosity) and the Capillary number (**Ca**) in eq. (**6**) but also on the injector volume (V_I) where the necking occurs between the injector (included) and the start of the collection channel. The volume of the droplet is also dependent on the dynamic viscosity (μ) and the flow rate (**Q**) ratios between the dispersed and the continuous phase. Finally, the volume depends on constant parameters **K**, β, η and α. The values of the parameters **K**, β, α and η are respectively 30.04, 1.812, 0.52 and 0.7 **[13]**.

$$V_{droplet} = K\frac{Ca^{\alpha-1}}{Re}\left(\frac{\mu_d}{\mu_c}\right)^{\eta} V_I \left(\frac{Q_d}{Q_c}\right)^{\beta} \tag{7}$$

2.2.2 Surface tension between the continuous and the dispersed phases

As mentioned in the introduction, the interfacial tension is a major concern in the droplet formation depending notably on the capillary number eq. (**6**). To estimate the size of droplets in a droplet generator chip, it is necessary to measure the interfacial tension. The interfacial tension measurement was performed by the stalagmometric method explained below the eq. (**8**).

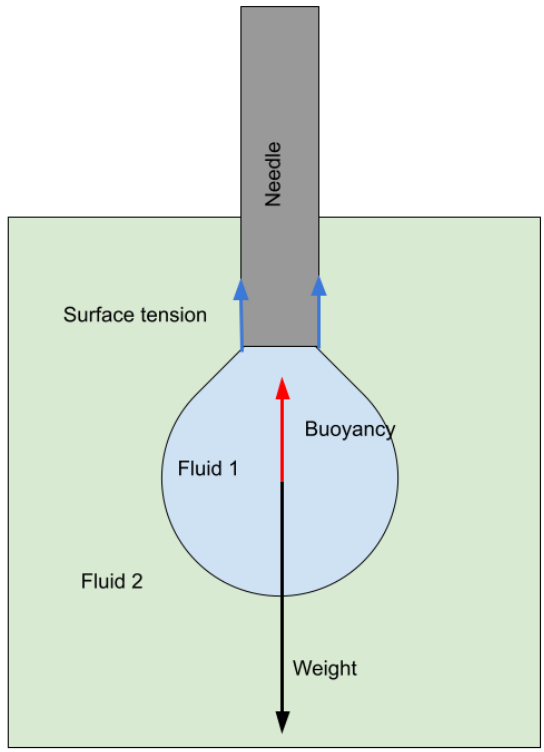

Figure 4: Diagram of the dripping from a needle. The forces in action on the droplet of the fluid 1 are the interfacial tension, the buoyancy and the weight. The interfacial tension applies at the interface fluid 1-fluid 2 and is represented here with blue arrows. The buoyancy and the weight apply to the center of gravity of the droplet and are represented respectively with red and black arrows.

From the scheme Fig. **4**, the eq. (**8**) of the interfacial tension (γ) between two fluids can be set. The interfacial tension depends on the density difference ($\rho_{fluid1} - \rho_{fluid2}$), the volume of the droplet ($V_{droplet}$) just before it falls and the inner radius (R_{in}) or the outer radius (R_{out}) of the needle. If the interfacial tension is strong enough, the droplet can grow onto the needle for small volumes. In that case, the outer radius is used to calculate the interfacial tension. However, if the droplet only grows down from the needle, the inner radius is chosen.

$$\gamma = \frac{(\rho_{fluid_1} - \rho_{fluid_2}) V_{droplet} g}{2\pi R_{in/out}} \tag{8}$$

The experimental process is the following. A syringe pump pushes the heavier fluid inside the lighter one. Droplets fall and the volume pushed is measured by the syringe pump. To reduce the uncertainty, several droplets are dripped and the total volume is then divided by the total amount of droplet produced. However this experiment to measure the interfacial tension is not perfectly accurate as only a part of the volume of the drop falls **[14]**. To check this assumption, the experiment was performed with water in air at 20°C. Without the correction factor, a surface tension of 99 ± 10 mN/m was measured. The real surface tension is 72.86 mN/m which is outside of the range of the experimental value even with the uncertainty. While multiplying by the correction factor which depends on the inner diameter of the syringe and the volume of the drop as $\frac{r}{V^{1/3}}$ as shown in Fig. **5**, we obtain a more accurate surface tension of 77.2 ± 7.8 mN/m.

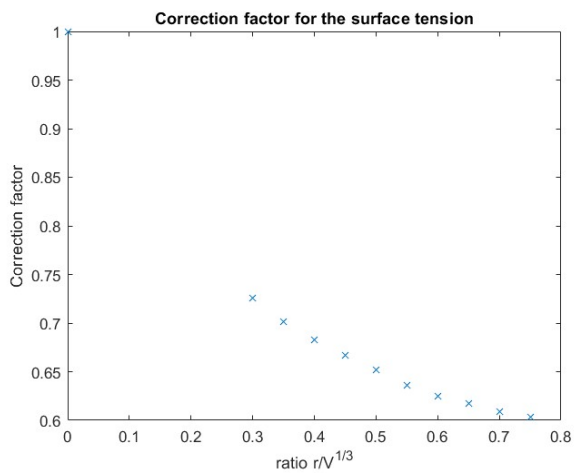

Figure 5: The correction factor corresponds to a correction of the partial droplet that falls from the needle. The values for the correction factor are taken from **[14]**.

The interfacial tension was measured for two solutions. Droplets of fluorinated oil with 2% Krytox are dripped in both solutions. One solution of water and 1.6wt/-vol% of agarose without any florescein and one solution with fluorescein. The idea here is to evaluate the influence of the fluorescein on the interfacial tension as it is used in the experiments to observe the droplet formation. The fluorescein particles emit light when lighted up with a LED which allows to observe the droplet formation through the microscope. It appeared that the fluorescein has a real impact on the interfacial tension between the fluorinated oil with 2% Krytox and the agarose solution.

Without the fluorescein, the droplets were going upward on the needle before dropping once the volume had increased enough (Fig. **6**). The interfacial tension with the method previously detailed was measured at $2.06 \pm 0.21\ mN/m$.

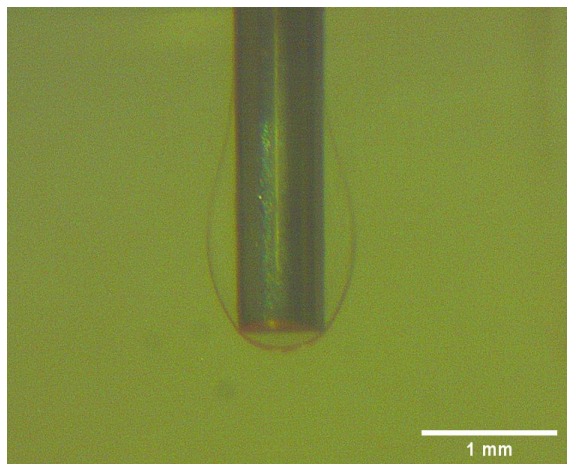

Figure 6: Dripping droplet of fluorinated oil with 2% Krytox into water with 1.6wt/vol% agarose and no fluorescein.

With the fluorescein, the droplets were growing downwards and were smaller (Fig. **7**). It could be that with fluorescein, the aqueous phase wets the steel whereas for the no fluorescein case, the oil wets the steel better. This competition results in a lower interfacial tension when fluorescein is used in the aqueous phase. The interfacial tension was measured at $0.0275 \pm 0.028\ mN/m$.

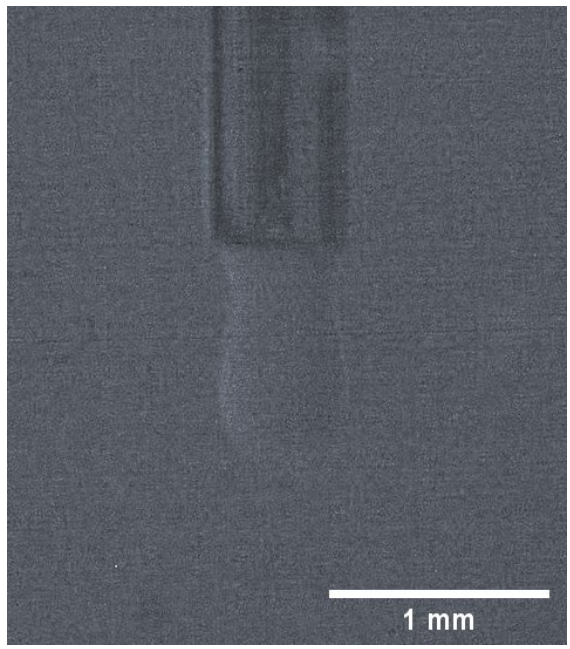

Figure 7: Dripping droplet of fluorinated oil with 2% Krytox into water with fluorescein and 1.6wt/vol% agarose.

2.3 Results

To estimate the size of the droplets generated with the different chips, different parameters were adjusted to the chip of the experiment. The characteristic length was chosen to be the smallest dimension in the chip being 10 µm for the Micronit chip and 30 µm for the 947 design from ChipShop.

A plot of the computational results from the model eq. (**7**) **[13]** for the two chips used (Appendix A and Appendix B) is given Fig. **8**. The flow rates were chosen to keep the system in the range of the dripping mode.

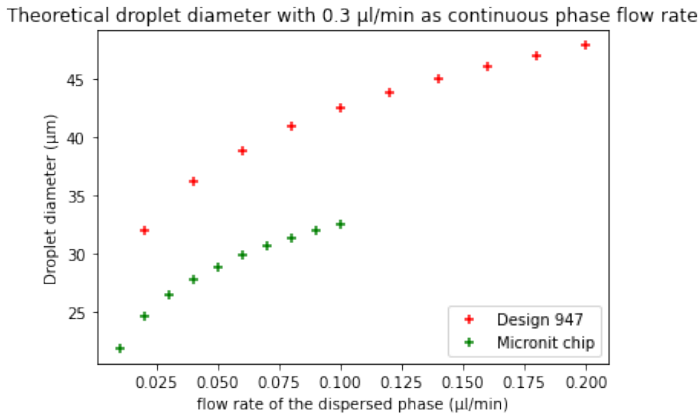

Figure 8: Droplet diameter depending on the dispersed phase flow rate for two different chips.

The η parameter of 0.7 leads to a parabolic curve (eq. (**7**)). The experiments to make water droplet in fluorinated oil showed relatively constant size for the droplets in the range of the dripping mode. The diameters of the droplets measured from the images (taken with the microscope) with imageJ did not change substantially with the flow rates (see more Fig. **13** and **14**). Besides, the estimated droplet diameters were about 23 µm for the 947 design and 10 µm for the Micronit chip which are lower than the values given by the theoretical model. Nevertheless, the optical setup should be improved to obtain more accurate values for the measured droplet size. However, a proper experimental process has not been done and it would need more experimental measurements to validate and/or improve the model. For different chip designs, chip materials and solutions the η constant parameters could very likely be modified. To conclude, this theoretical droplet size model could be interesting to manage the droplet size production but the lack of experimental validation makes it incomplete so far.

3 Gel particles generation

3.1 Agarose gel production and properties

Agarose is a polysaccharide which contains mostly galactose monomeres. The agarose is among others used to make gel for electrophoresis. The gel has a porous structure which means, the medium around the gel diffuses in changing its properties (density, compressibility). Either, the gel is filled with a solution which does not diffuse out and it has fixed properties or the properties could change with the medium used replacing the existing solution inside the pores of the gel. The experimental agarose gel is simply made with water and agarose powder. The agarose powder used in this project is the *ultra-low gelling temperature agarose a5030* from Sigma Aldrich. In this part, the protocol to make the agarose solution will be detailed. Some interesting properties of the solution are also investigated. The experiments presented in this part will give suggestions on how the agarose solution can be used in further experiments.

3.1.1 Agarose gel production protocol

As mentioned in section **1.4.3**, the agarose powder structure is held together with hydrogen bonds. To make agarose solution, these hydrogen bonds need to be broken. Once the agarose powder is mixed with water, the solution is heating up (in a water bath at about 80°C for 1 hour) to break the hydrogen bonds of the agarose powder and release the agarose molecules into water. To ensure the homogeneity of the agarose solution, the solution is stirred each 10 minutes.

After one hour when the agarose molecules are well dissolved into the water, the solution can be taken out of the water bath. If now the solution reaches the gelling point, the hydrogen bonds occur between different molecules. There are water-water hydrogen bonds, agarose-agarose hydrogen bonds and finally water-agarose hydrogen bonds. These hydrogen bonds between the molecules of water and agarose, represented in Fig. **9**, are responsible for gelling of the solution at lower temperature **[15]**. The solution can be melted and gellified multiple times as molecules of water and agarose will always be bind with an hydrogen bond around the gelling temperature.

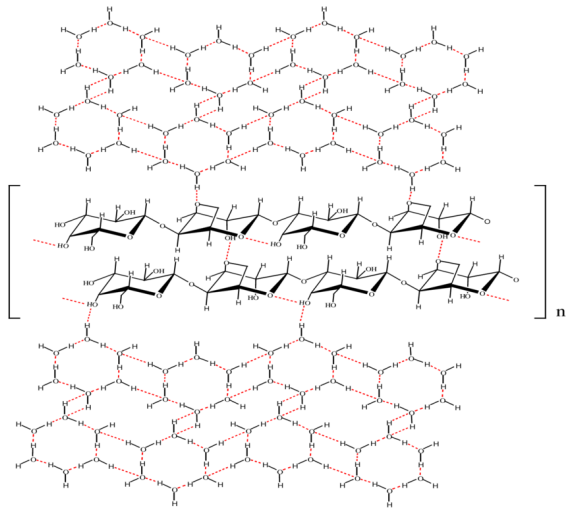

Figure 9: Molecules of agarose and water held together with hydrogen bonds represented in red dotted lines. **[15]**

3.1.2 Hysteresis change of states of the agarose gel

One of the very interesting properties of the agarose gel is the hysteresis change of states with temperature. Indeed, there is a range of temperature where the gel is stable. Once the gel is formed, the solution needs to be heated higher than the gelling point to break the hydrogen bonds and be melted.

This hysteresis behavior is useful for two main reasons. The first reason is for the gel particles generation. Once melted, the solution is used to generate gel particles at a temperature about the room temperature. For some concentrations the solution stays in a liquid form over some period which allows the gel droplet formation. This is detailed in the section **3.1.3**. The second reason is for the conservation of the gel particles. Once, the particles are generated and gellified, they are stable at room temperature. It is then possible to conserve them under normal conditions and use them in most of the acoustofluidic experiments since the temperature is generally about the room temperature.

3.1.3 Viscosity of the agarose gel

The dimensions of the droplet generator chips used to generate gel particles are in the micrometer range. As a result, the pressure in the channels is intrinsically already high. Besides, the agarose gel can have a high viscosity. This high vis-

cosity would increase even more the pressure needed for the solution to flow in the channels. It is therefore very important to keep the viscosity of the gel as low as possible. The viscosity solutions with different agarose concentrations and different viscosities are investigated. The solution is turned into liquid form and then cooled down to room temperature. Then the viscosity of the solution is measured steadily to see how it evolves with time at room temperature.

The viscometer used is the Minivis II from Grabner instruments. The viscosity of the solution is measured with a falling ball to estimate the drag force applied by the liquid on the ball. The other forces which apply to the ball are the weight and the buoyancy. A scheme of these forces is represented Fig. **10**. The eq. (**9**) gives the dynamic viscosity μ of the fluid depending on the density of the ball ρ_b, the density of the fluid ρ_f, the velocity of the ball **v**, the gravity constant **g** and the radius **R** of the ball. The equation is valid only if the walls are far from the ball which is not the case in this device. For this reason, the device must be calibrated for a given ball in a fluid with well-known properties to adjust a calibration coefficient. For most cases, the water is the liquid used to calibrate the device when the viscosity remains quite low. However, when the viscosity becomes higher, smaller balls are used and the water can no longer be used to fit the parameters of the ball. This situation happened with the agarose gel and the device had to be calibrated with a smaller ball in glycerol with water. The viscosity of the water with glycerol is higher than water and can be adjusted as desired. The density and viscosity of water with glycerol for different concentrations is tabulated **[16]**.

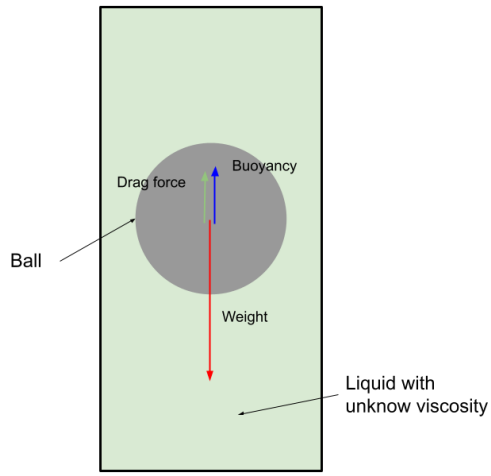

Figure 10: The ball falls through the solution with unknown viscosity. The forces in action are the weight that drags the ball down, the drag force pushing the ball to the opposite direction of the motion and the buoyancy with an opposite direction with the gravity force.

$$\mu = \frac{2}{9}\frac{\rho_b - \rho_f}{v} g R^2 \tag{9}$$

The viscosity of 3 different agarose solutions with different concentrations is measured. The concentration of the solutions is 1%wt/vol, 1.6%wt/vol and 2%wt/vol agarose in water. Each solution is heated up to turn the gel into liquid form. The viscosity measurement begins once the solution reached the room temperature of about 25°C. The viscometer measures the viscosity of the solution for a certain time every 5 minutes in average. The results are displayed in the Fig. **11**.

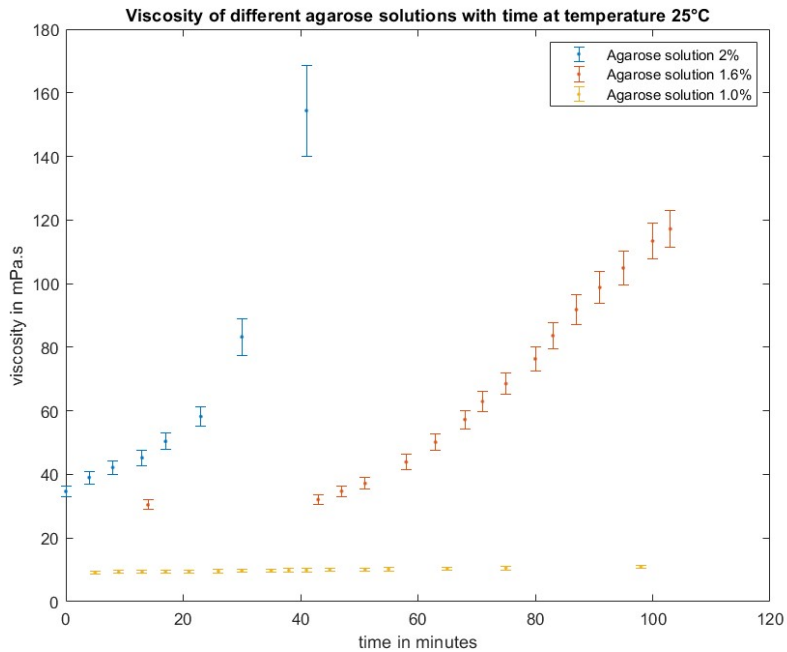

Figure 11: The viscosity of the agarose solutions changes through time at the temperature of 25°C. Three solutions with different concentrations are displayed. The measurement errors are evaluated and placed as error bars on the graph.

From the Fig. **11**, the viscosity of each solution seems to be relatively stable for a period which depends on the concentration before it rises. The higher the agarose concentration is and the lower this time is before the viscosity increases. As the flow rate for the droplet generation remains low, the reasonable time to make particles needs to be around an hour. For a flow rate of 0.05 $\mu l/min$ for the dispersed phase during one hour, the volume produced is about 3 μl. However, the solution with 1 wt/vol% agarose produces soft particles that break up more easily. Which is why the choice of 1.6 wt/vol% agarose concentration has been made to be able to produce particles for a certain amount of time and in the same time obtain particles strong enough not to break up. Some improvement in the setup would need to be implemented to keep the solution at a given temperature all along the path and get a steady viscosity during the particle production. One can think of a temperature controller on the syringe and the tubing for instance.

3.2 Microfluidic generation of gel particles

3.2.1 Setup and method

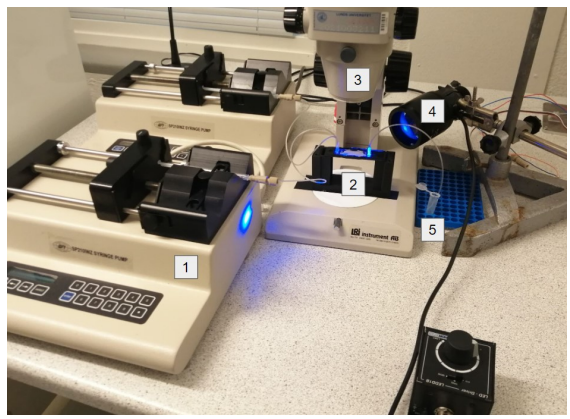

Figure 12: Setup to generate droplets to make gel particles. The syringe pumps (1) control the flow rates in the *Focused flow droplet generator - topconnect* chip (2). The stereo microscope (3) allows to image the particles thanks to the blue LED (4) which has the wavelength to activate the fluorescein in the solution. Finally the droplets are pushed out of the chip in a tank (5) to be cooled down and transform into gel.

As mentioned above, the flow rates in the chip are adjusted to be in the dripping mode. Once the flow is steady, the agarose droplets are collected in the tank. The setup of the experiment is given in the Fig. **12**. Several parameters make the droplet generation difficult. Among the problems it is possible to face, there is (1) the high pressure due to the very small dimensions of the tubings and the chip design. Some tubings tend to disconnect if the pressure is too high. (2) The hydrophobic material of the chip is sometimes also not perfect (especially for the *Fluidic 947*). It happens that the dispersed phase sticks to the wall disturbing the flow and thus the droplet generation. The last main problem (3) comes with the collection of the droplet. They tend to merge once collected in the tank.

3.2.2 Droplet generation with 30 µm-injector chip

The 30µm-injector chip (*Fluidic 947*) from microfluidic ChipShop GmbH is made with TOPAS material which is hydrophobic. The design of the chip is given in Appendix **A**. The advantage of the natural hydrophobic properties of the material

is that it does not need treatment to produce water droplets in oil. For instance, the use of Repel-silane in glass chip coat the glass material to make it hydrophobic. However the hydrophobic properties of TOPAS are not perfect which means the water phase tends to stick to the walls. This drawback prevents the steady droplet generation needed to produce gel particles consistently.

Droplets are generated with a flow rate of 0.3 $\mu l/min$ for the continuous phase and 0.1 $\mu l/min$ for the dispersed phase. The flow rates is generated with syringe pumps shown in Fig. **12**. The size of the droplets on Fig. **13** is in average 23 μm diameter. It was measured using the imageJ software with the scale calibration on the width of the channel.

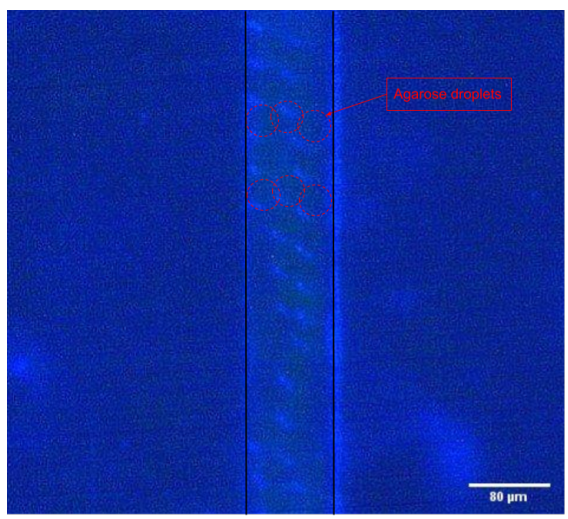

Figure 13: Droplet generated with the *Fluidic 947* chip from ChipShop. The water phase is a 1.6wt/vol% agarose in water and the continuous phase is a fluorinated oil HFE-7500 with 2% Krytox.

3.2.3 Droplet generation with 10 µm-injector chip

To get even smaller particles and get closer to the real size of a white or red blood cell, the *Focused flow droplet generator - topconnect* with 10 µm-injector from Microcnit was chosen. This chip is made of glass coated to have a hydrophobic surface. Repel-silane can be used to give hydrophobic properties back to the chip once it lost it. The solution is push in the chip to fill the channels. After a couple of minutes, the Repel-silane is flushed out of the chip with some water.

Droplets are generated with a flow rate of 0.3 $\mu l/min$ for the continuous phase and 0.05 $\mu l/min$ for the dispersed phase. The size of the droplets on Fig. **14** is in

average 10 μm diameter.

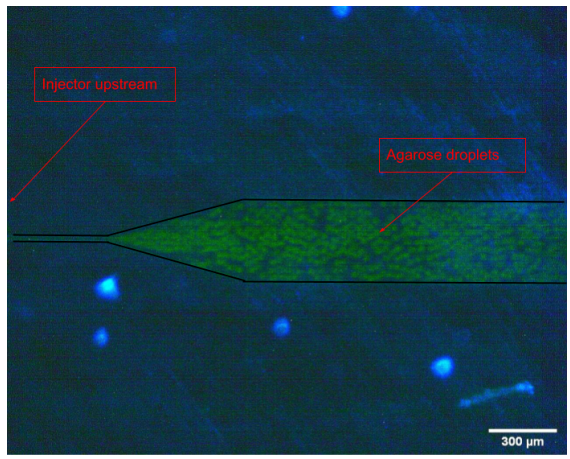

Figure 14: Droplet generated with the *Focused flow droplet generator - topconnect* with 10 µm-injector from Micronit. The water phase is a 1.6wt/vol% agarose in water and the continuous phase is a fluorinated oil HFE-7500 with 2% Krytox.

3.2.4 Collection, rinsing and storage of the droplets

To collect the droplets I tried different techniques. (1) I first put the tubing connecting the outlet and the collection tank in an ice bath. However it seemed to disrupt the droplets which all merged once reaching the part of the tubing in the ice bath. (2) I also tried to use a Peltier element to keep the chip at ambient temperature upstream of the injector and to cool down the chip around 10°C downstream of the injector. The idea here was to produce the droplets and form the gel structure directly in the channel. However, once again it was not conclusive as the droplets remain in the channel for few seconds before leaving the chip through the outlet and it takes more time than this to form the gel structure. So the easiest way to collect the droplets was (3) to keep all the setup working at ambient temperature while collecting the agarose droplets in the liquid form. Then either the sample was held for some time (about one hour) at the ambient temperature to obtain the gel structure or was put in the fridge to be cooled down to transform the agarose droplets into gel more rapidly. In the fridge, as well as the ice bath, the droplets sometimes merged probably due to the cold temperature.

Once gel particles are collected and formed, the fluorinated oil collected with the sample must be replaced by an aqueous phase. The gel particles collected on top of the oil phase are pipetted and transferred into in a solution of water with a small

amount of Krytox 157 FSL as surfactant (around 2 wt/vol%). The surfactant is used here to remove the last fluorinated oil residues around the particles. The agarose density of 1.64 g/ml **[17]** is higher than the water so the gel particles are supposed to sink in the water which is the behavior observed. As the amount of agarose was arond 2 wt/vol%, the density of a gel particle is about 1.01 g/ml. Because the fluorinated oil is heavier than this density ($\rho = 1.61\ g/ml$ for the fluorinated oil used in this thesis), it is difficult to check whether the gel particles are still filled and/or surrounded by some fluorinated oil. Indeed, they would sink in the water faster or slower, with or without oil but it could not be possible to judge by eye with these small amount of particles. Another way of rinsing the gel particles could be to use centrifugal forces. The centrifugal force is stronger for particles with a higher density. The droplet collection would need the use of an aqueous phase with a higer density then the droplet but lower than the oil. The iodixanol gradient shown in Fig. **15** has a maximum density around 1.2 g/ml. So the density of the aqueous phase that should be used need to be higher than this value. The other issue with this technique is that it does not guarantee the oil potentially inside the pores of the gel particles to be removed.

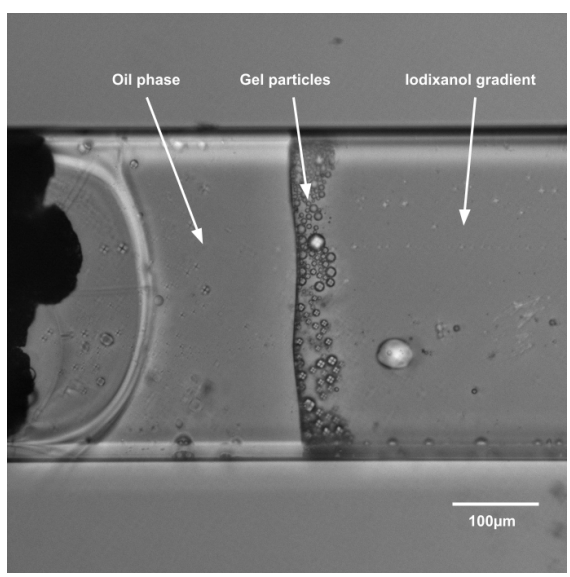

Figure 15: Image of the capillary after centrifuging. The agarose gel particles are heavier than the maximum density of the iodixanol (1.2 g/ml). There are still some oil with the gel particles they were removed from the oil phase with the pipette.

4 Acoustophoresis experiments with gel particles

4.1 Setups and Method for the acoustofluidic experiment of the gel particles

The acoustic behavior of the gel particles is investigated with an acoustofluidic chip (cross section of 375 μm and depth of 150 μm). Water is chosen to be the medium for the experiment to keep the droplets in the same fluid without risking any destruction of the sample. The experiment is performed in stop flow because of the small amount of gel particles available. Droplets are taken into a syringe and pushed with the syringe pump until some droplets are observed in the acoustofluidic chip. One of the chips (channel wet etched glass on silicon) used is shown in Fig. **16**. Once the flow stopped, the function generator is set to 2 MHz to activate the piezo-element (piezo pzt) and create the standing acoustic half-wave in the cross section of the channel. Videos of the motion of the particles are taken with the Nikon microscope showed in Fig. **17**.

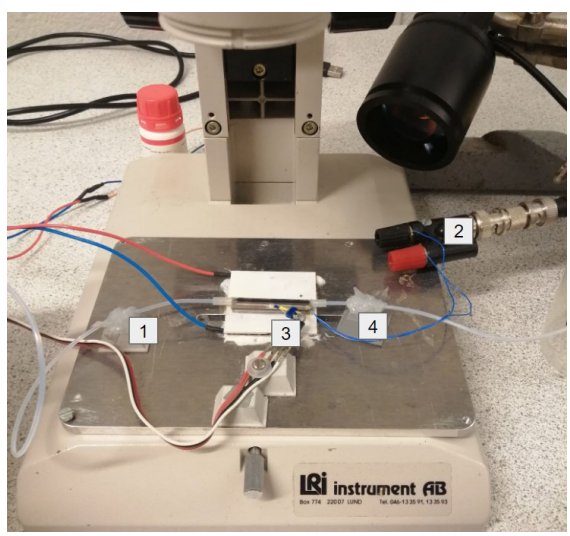

Figure 16: The solution containing the gel particles is inserted in the chip through the inlet tubing (1). A function generator creates a 2MHz periodic sinusoidal function (2) to trigger the piezo-element below the chip (3) and create the standing sound half-wave in the channel. The wave function is displayed on the oscilloscope to check the shape and the frequency of the signal. The waste is driven out of the chip through the outlet (4)

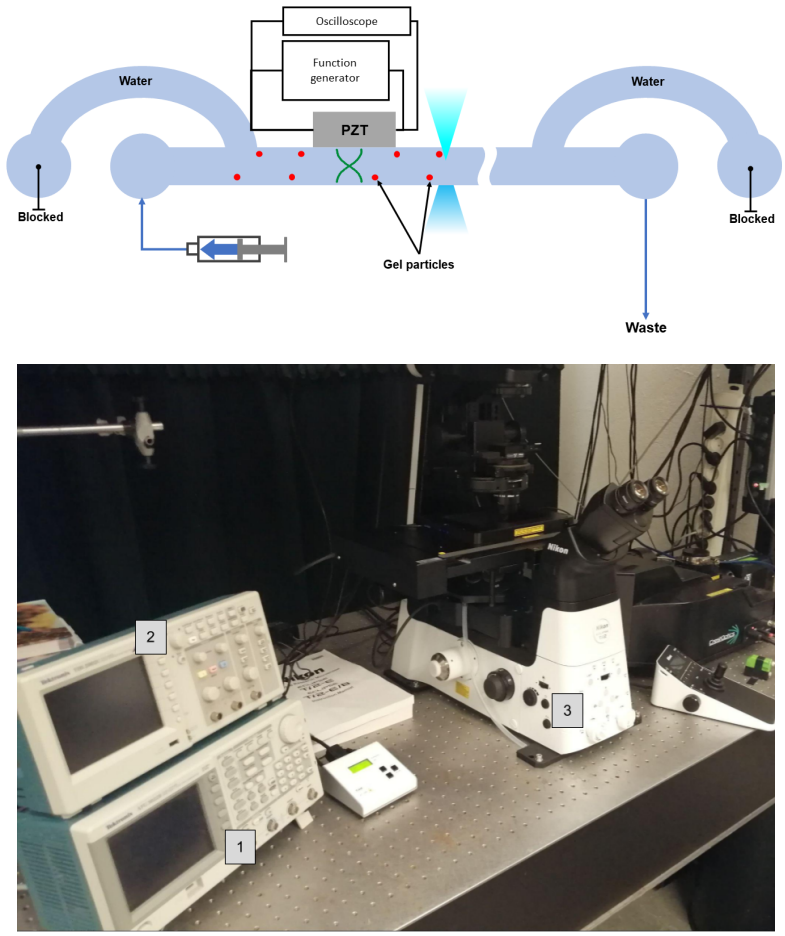

Figure 17: Schematic diagram of the acoustofluidic setup on top. Below an image of the instruments with the function generator (1), the oscilloscope (2) and the microscope (3)

For practical reason concerning the quality of the images, the experimental images given in the Results section are obtained with the setup Fig. **17**.

4.2 Experimental results

The images of the gel particles in Fig. **18** and **19** are taken with the Nikon Eclipse Ti2-E. Different behaviors of the gel particles in the acoustofluidic system have been observed with the experiments performed on two different samples. The gel particles sample was produced with the 10 µm injector chip from micronit. The

particles of one sample (bright ones in the image (a) of the Fig. **18**) are pushed to the anti-node when the sound wave is active in the channel. The intensity standard deviation (from the imageJ software) of all the images from the video shows the path taken by the particles (from their initial position to the walls). These particles have a size between 7 μm and 10 μm. However particles from another sample that are seen as gray blurry particles in the background of the image (a) of the Fig. **19** circle around in the acoustic streaming which is imaged by the intensity standard deviation in the bottom picture. The size of these particles is about 7 μm. After a certain time, a black cluster of particles seems to be focused in the center of the channel when the sound wave is activated.

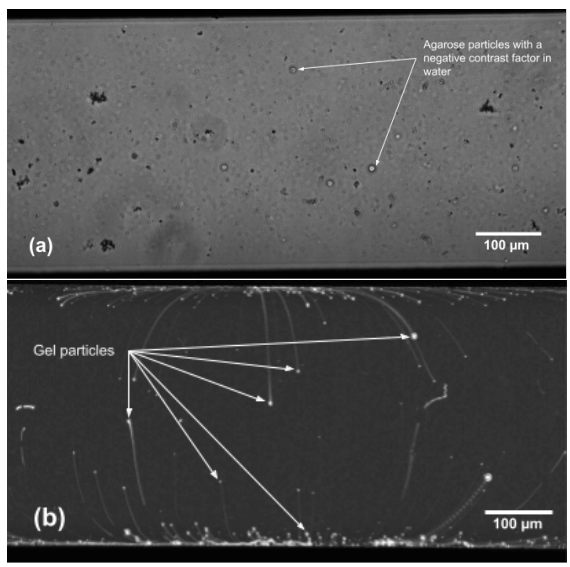

Figure 18: The top picture (a) is one image from the video taken with the Nikon Eclipse Ti2-E microscope. The bottom picture (b) is the intensity standard deviation taken from all the images of the video. Every particle motion is directed to the walls.

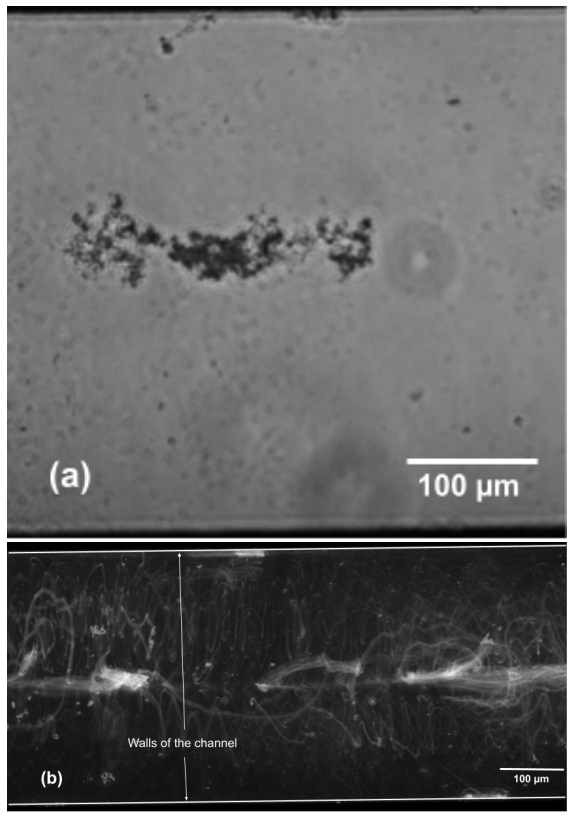

Figure 19: The top picture (a) is one image from the video taken with the Nikon Eclipse Ti2-E microscope. It shows the black cluster and also shows circulating particles in the blurry background. The bottom picture (b) is the intensity standard deviation taken from all the images of the video. The black cluster from (a) can be observed in the bright cluster on the left part of (b). Particles have a chaotic motion circulating in the vortices.

4.3 Discussion and perspectives

First of all, the black cluster in the top picture of the Fig. **19** seems visually to be collapsed gel particles gathering in the center of the channel with the sound wave. Indeed, the gel particles are fragile and tend to break up sometimes. The two Figures **18** and **19**, clearly show that the gel particles interact with the acoustic field in the water medium. However, different behaviors have been observed in the experiments performed. Either the particles are pushed to the anti-node or they are circulating in the acoustic streaming created by the acoustic wave. A first reasonable assumption

is that the gel particles in Fig. **19** are too small or the contrast factor too small and the acoustic radiation force is to weak to compensate the force induced by the acoustic streaming. Besides, in Fig. **18**, it could be that some fluorinated oil is still surrounding the gel particles changing their acoustic properties and increasing the radiation force experienced by them. The compressibility of the fluorinated oil could be measured to evaluate its contrast factor in water and check the behavior of this oil under the acoustic radiation force. It would also be possible to add some hydrophobic fluorescent dye that would stay in the oil phase and could help to detect any potential remaining oil in or around the gel particles.

To draw a conclusion about the experiments performed, the gel particles cannot seemingly be tuned in a large range by varying the agarose concentration because of the rapid viscosity increase for higher concentrations. Secondly, even for the concentration used in this work, the experimental time is limited with such setups (about one hour). So the production rate is somewhat limited (33 hours to produce 1ml of agarose particles). Otherwise, it was shown that gel particles are sensible to the acoustic radiation force when the medium used is water. Besides it has been possible to produce particles in the size range of the human red and white blood cells. It is however not possible to give the exact behavior and acoustic properties of the gel particles as different phenomena have been observed. To avoid the circulating particles into the acoustic streaming, the solution is to make bigger particles and thus increase the acoustic radiation force on them. Finally, it is necessary to find a way of getting rid of the fluorinated oil surrounding the gel particles which obviously changes the acoustic properties. The measurement of the acoustic properties of the fluorinated oil used seems to be mandatory to be able to understand deeper how the droplets would behave with and without oil.

Appendix A

Design of the chipchop *Fluidic 947*

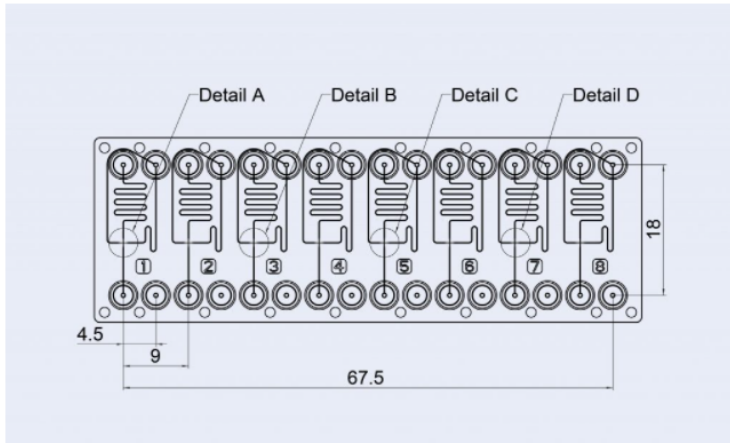

Dimensions of Fluidic 947

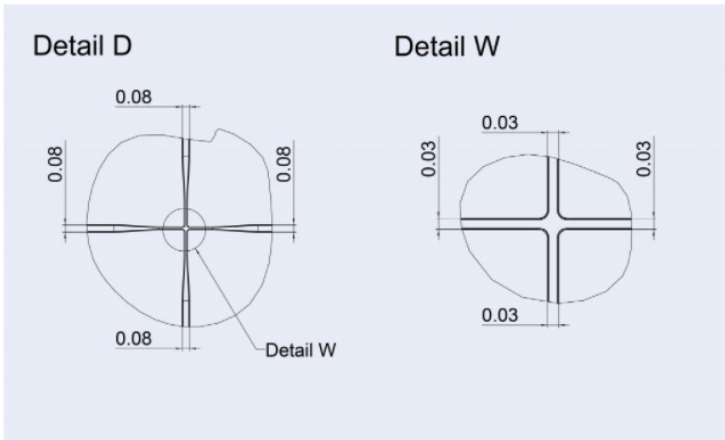

Detail D of Fluidic 947

Appendix B

Design of the micronit *Focused flow droplet generator - topconnect* with 10µm nozzle

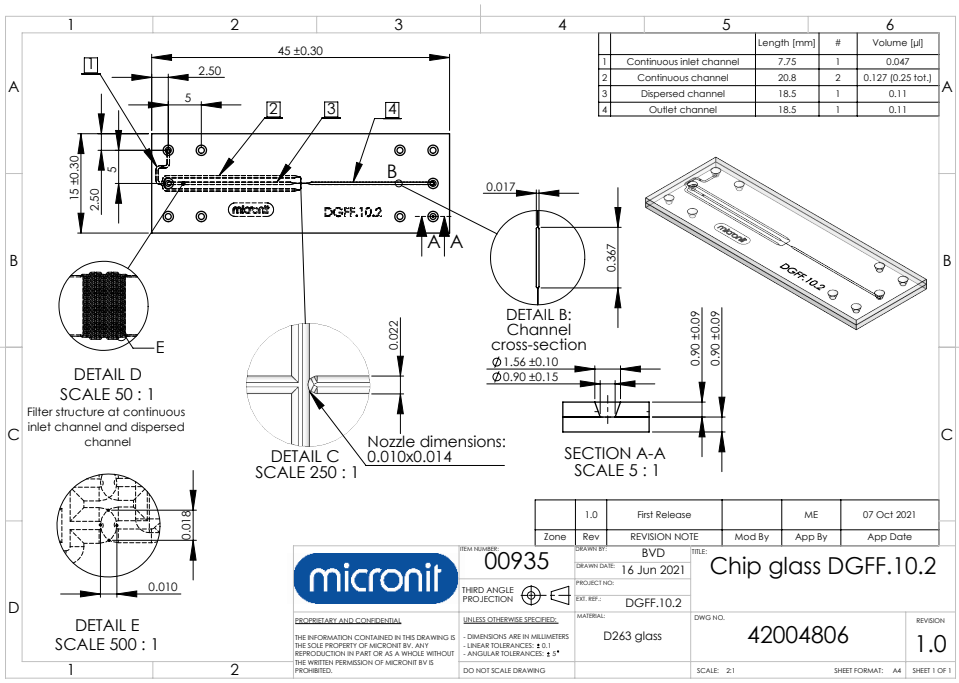

		Length [mm]	#	Volume [µl]
1	Continuous inlet channel	7.75	1	0.047
2	Continuous channel	20.8	2	0.127 (0.25 tot.)
3	Dispersed channel	18.5	1	0.11
4	Outlet channel	18.5	1	0.11

References

[1] Per Augustsson. *On microchannel acoustophoresis Experimental considerations and life science applications Doctoral thesis*. 2011.

[2] Per Augustsson et al. 'Iso-acoustic focusing of cells for size-insensitive acousto-mechanical phenotyping'. In: *Nature Communications* (2016). DOI: 10.1038/ncomms11556.

[3] 'Microfluidic preparation of monodisperse polymeric microspheres coated with silica nanoparticles'. In: *Scientific Reports* (Dec. 2018). DOI: 10.1038/s41598-018-26829-z.

[4] Sami Sahin and Karin Schroën. 'Partitioned EDGE devices for high throughput production of monodisperse emulsion droplets with two distinct sizes'. In: *Lab Chip* (Apr. 2015). DOI: 10.1039/C5LC00379B.

[5] Eugenia Cifuentes et al. 'Synchronized prostate cancer cells for studying androgen regulated events in cell cycle progression from G1 into S phase'. In: *Journal of Cellular Physiology* (2003). DOI: 10.1002/jcp.10317.

[6] Hui Sung Moon et al. 'Continual collection and re-separation of circulating tumor cells from blood using multi-stage multi-orifice flow fractionation'. In: *Biomicrofluidics* (2013). DOI: 10.1063/1.4788914.

[7] Cushing Kevin et al. *Reducing WBC background in cancer cell separation products by negative acoustic contrast particle immuno-acoustophoresis | Elsevier Enhanced Reader*. 2018. DOI: https://doi.org/10.1016/j.aca.2017.11.064.

[8] Matthew C. Blosser, Benjamin G. Horst and Sarah L. Keller. 'CDICE method produces giant lipid vesicles under physiological conditions of charged lipids and ionic solutions'. In: *Soft Matter* (2016). DOI: 10.1039/c6sm00868b.

[9] 'Giant liposome formation toward the synthesis of well-defined artificial cells'. In: *Journal of Materials Chemistry B* (2017). DOI: 10.1039/c7tb01322a.

[10] Björn Stenestam. *Examensarbete 30 hp Acoustic trapping of sub-micrometre particles within microfluidics*. 2003. URL: http://www.teknat.uu.se/student.

[11] Anna Fornell et al. 'An acoustofluidic platform for non-contact trapping of cell-laden hydrogel droplets compatible with optical microscopy'. In: *Biomicrofluidics* (2019). DOI: 10.1063/1.5108583.

[12] Axel Happstadius. *Acoustic Trapping of Droplets*. 2018.

[13] Katerina Loizou, Voon Loong Wong and Buddhika Hewakandamby. 'Examining the effect of flow rate ratio on droplet generation and regime transition in a microfluidic t-junction at constant capillary numbers'. In: *Inventions* (2018). DOI: 10.3390/inventions3030054.

[14] D Wieeiam Harkins and F E Brown. *Surface tension of water and Benzene-499 the determination of the surface tension*. 2022. URL: https://pubs.acs.org/sharingguidelines.

[15] Masakuni Tako et al. 'The Principles of Starch Gelatinization and Retrogradation'. In: *Food and Nutrition Sciences* (2014). DOI: 10.4236/fns.2014.53035.

[16] W. L. Hill, H. L. Marshall and K. D. Jacob. 'Composition of Crude Phosphoric Acid Prepared by Sulfuric Acid Process'. In: *Industrial & Engineering Chemistry* (1932). DOI: 10.1021/ie50273a023.

[17] Alain Pluen et al. 'Diffusion of Macromolecules in Agarose Gels: Comparison of Linear and Globular Configurations'. In: *Biophysical Journal* (1999). DOI: https://doi.org/10.1016/S0006-3495(99)76911-0.